

Fractographic Study of Adhesion Tested Thermal Barrier Coatings Subjected to Isothermal and Cyclic Heat Treatments

Robert Eriksson, Håkan Brodin, Sten Johansson, Lars Östergren and Xin-Hai Li

Linköping University Post Print



N.B.: When citing this work, cite the original article.

Original Publication:

Robert Eriksson, Håkan Brodin, Sten Johansson, Lars Östergren and Xin-Hai Li, Fractographic Study of Adhesion Tested Thermal Barrier Coatings Subjected to Isothermal and Cyclic Heat Treatments, 2011, Procedia Engineering, (10), 195-200.

<http://dx.doi.org/10.1016/j.proeng.2011.04.035>

Copyright: Elsevier. Under a Creative Commons license

<http://www.elsevier.com/>

Postprint available at: Linköping University Electronic Press

<http://urn.kb.se/resolve?urn=urn:nbn:se:liu:diva-70541>

ICM11

Fractographic study of adhesion tested thermal barrier coatings subjected to isothermal and cyclic heat treatments

R. Eriksson^{a,*}, H. Brodin^{b,a}, S. Johansson^a, L. Östergren^c, X.-H. Li^b

^aDivision of Engineering Materials, Linköpings universitet, SE-58183 Linköping, Sweden

^bSiemens Industrial Turbomachinery AB, SE-61283 Finspång, Sweden

^cVolvo Aero Corporation, SE-46181 Trollhättan, Sweden

Abstract

Thermal barrier coatings (TBC) are used in gas turbines to protect metallic components from high temperature. In the present study adhesion tests have been conducted on APS TBC coated specimens subjected to different heat treatments. Isothermal and cyclic heat treatments have been conducted at temperatures around 1100 °C and the adhesion have been tested using the method described in *ASTM C633*. The fracture surfaces resulting from the adhesion test have been investigated and the fracture behavior has been characterized. A difference in fracture mechanism between the three heat treatments has been found. The two cyclic heat treatments give fracture in the top coat/bond coat interface while isothermal heat treatment gives fracture in the top coat.

© 2011 Published by Elsevier Ltd. Selection and peer-review under responsibility of ICM11

Keywords: thermal barrier coatings; TBC; adhesion; fractography; thermal cycling fatigue; burner rig test

1. Introduction

Since the combustion temperature in gas turbines exceeds that which metallic materials can handle, structural elements in the hot parts of a gas turbine are often protected by thermal barrier coatings (TBC). Thermal barrier coatings consist of a ceramic top coat (TC), which provides insulation, and a metallic bond coat (BC) to improve bonding and oxidation resistance. The TC typically consists of 7–8 % Y₂O₃-stabilized-ZrO₂ and the BC usually consists of MCrAlY where M is metals such as Ni and Co, [1]. A common method for deposition of TBCs is air plasma spraying (APS). During high temperature exposure

* Corresponding author. Tel.: +46 13 284410; fax: +46 13 282505.

E-mail address: robert.eriksson@liu.se

the BC will oxidize and form thermally grown oxides (TGO). The first TGO to form will consist mainly of Al_2O_3 ; as Al is depleted from the BC, other oxides will form: $(\text{Al}, \text{Cr})_2\text{O}_3$, NiO or spinel type $(\text{Ni}, \text{Co})(\text{Al}, \text{Cr})_2\text{O}_4$, [2, 3].

Adhesion testing, (or fracture toughness testing), of TBC is one of the methods available for characterizing the durability of TBCs, [4-6]. Fracture situated around the TGO will appear dark to the eye and are referred to as *black fracture*; fracture that occur in the TC is referred to as *white fracture*, [2]. Fracture surfaces often display a *mixed-type fracture* where both types of fracture mechanisms, black and white, are present. In the present study, adhesion tests have been conducted on as-sprayed and heat treated TBC coatings deposited on Ni-base substrates. The fracture surfaces resulting from the adhesion test have been further analyzed to study the fracture mechanisms.

2. Experimental

The studied specimens consist of APS deposited TBC on disc-shaped substrates of the Ni-base alloy Hastelloy X with a diameter of 25 mm and a thickness of ~6 mm. The substrate discs were coated with 150 μm of NiCoCrAlY with ~12 % Al and 300 μm of 7 % yttria-stabilized-zirconia.

The specimens were subjected to three different heat treatments: isothermal oxidation, thermal cycling fatigue (TCF) and burner rig test (BRT). The isothermal oxidation was conducted at 1100 °C for 1, 23, 47, 111 and 290 h. Thermal cycling fatigue was performed for 24, 48 and 300 cycles. One cycle consists of high temperature exposure at 1100 °C for 60 min followed by cooling by compressed air for 10 min, reaching a minimum temperature of 100 °C. Burner rig test was performed for 300 and 1150 cycles. One cycle consists of 75 s heating on the coated side by propane burners followed by 75 s of cooling on the uncoated side by air; the equipment is further described in [7]. A steady-state thermal analysis, using finite element software, predicts that the BC temperature will reach a maximum of ~1140 °C.

The heat-treated specimens were subjected to adhesion tests using *ASTM C633 Standard Test Method for Adhesion or Cohesion Strength of Thermal Spray Coatings*, [8]. The method involves fastening the specimen to two rods using epoxy adhesive, enabling the specimen to be mounted in a tensile test machine and loaded to fracture.

The fracture surfaces resulting from the adhesion test were analyzed in scanning electron microscope (SEM). The amount of black fracture was measured using energy dispersive scatter (EDS) mapping. For each specimen 18 1.30 x 0.98 mm maps were acquired for Ni, Co, Cr, Al, and Zr. The area fraction of Zr has been considered to correspond to the fraction of white fracture and the area fraction with combination of Ni, Co, Cr and Al has been considered to be black fracture. Microscopy studies were performed with a *FEG-SEM Hitachi SU-70* equipped with an EDS detector from *Oxford Instruments*. Before analysis in SEM, the specimens were coated with approximately 25 nm of carbon.

3. Results

3.1. Microstructure

The splat-on-splat structure gives rise to two kinds of discontinuities in the TC microstructure: between-splat delaminations and through-splat microcracks, as can be seen in Fig. 1 a). The through-splat microcracks can also be seen as a crack network in Fig. 2 a). When exposed to high temperature the TC starts to sinter, as shown in Fig. 1 b), where, especially the microcracks, can be seen to close by sintering. The extent of sintering is very similar for isothermal oxidation and TCF, but considerable lower in the case of BRT.

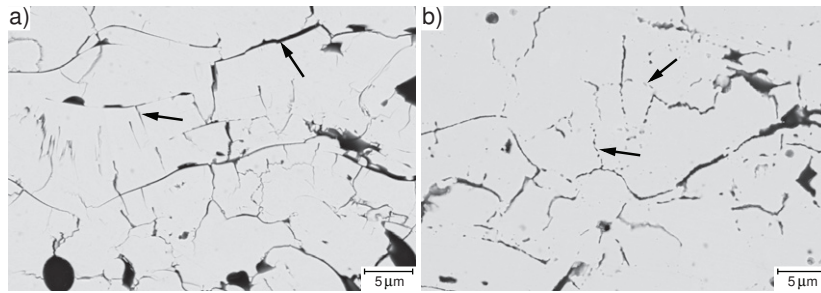


Fig. 1. Microcracks and delaminations in the top coat, SEM backscatter electron images. a) An as-sprayed specimen, arrows mark vertical through-splat microcracks and horizontal between-splat delaminations. b) Evidence of sintering in specimen subjected to 290 h of isothermal oxidation at 1100 °C, arrows mark sintered cracks.

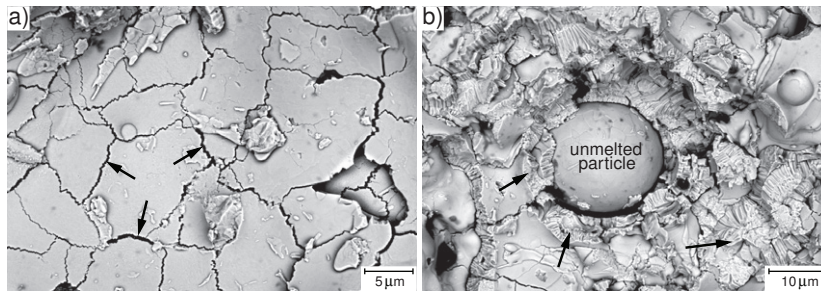


Fig. 2. Characteristics of white fracture, as-sprayed specimen; SEM backscatter electron images. a) A large area of interlamellar fracture, arrows mark the network of through-splat microcracks. b) Translamellar cracking, marked with arrows, associated with an unmelted particle.

The thickness of the developed interface TGOs in the specimens tested by isothermal oxidation and TCF are very similar. The composition of the interface TGO is the same for isothermal oxidation and TCF; it consists of mainly Al_2O_3 , occasionally crowned by $(\text{Cr}, \text{Al})_2\text{O}_3$ or spinels. In some areas in the BC/TC interface, bulky clusters of oxides have formed containing the full spectrum of oxides: Al_2O_3 , $(\text{Cr}, \text{Al})_2\text{O}_3$, spinels and NiO. The interface TGO thickness for the BRT-subjected specimens is considerable thinner than for isothermal oxidation and TCF. The composition of the TGO is mainly Al_2O_3 ; Cr-rich oxides and bulky oxide clusters are uncommon.

3.2. Adhesion test

Isothermal oxidation increased the adhesion of the TBC compared to the as-sprayed condition. The adhesion (fracture stress) of the isothermally heat treated specimens remained essentially constant, or increased slightly, throughout the testing, whereas the two cyclic heat treatments gave decreasing adhesion with increasing number of cycles; specimens subjected to BRT gave somewhat lower adhesion than specimen subjected to TCF.

The isothermally oxidized specimens gave essentially all white fracture for all oxidation times, as seen in Fig. 3 a), whereas both cyclic heat treatments gave increasing fraction of black fracture with number of cycles, Fig. 3 a). Fig. 3 b) shows a TCF-subjected specimen where the many areas of black fracture can be seen to range in size from $\sim 100 \mu\text{m}$ to $\sim 1 \text{ mm}$. The as-sprayed condition gave the highest fraction of

black fracture; however, the fracture mechanism changes from mixed fracture to white fracture after just 1 h of heat treatment, as seen in Fig. 3 a).

3.3. Characteristics of white fracture

The characteristics of white fracture is shown in Fig. 2. Regardless of heat treatment, the fracture surface consists mainly of large areas of interlamellar fracture (fracture between splats), shown in Fig. 2 a). The interlamellar cracks are formed from the preexisting delaminations between splats. There are a few examples of translamellar (trough–splat) fracture. These cracks can usually be associated with certain features in the microstructure, as in the case shown in Fig. 2 b) where an unmelted particle has caused extensive translamellar cracking in its vicinity. Translamellar cracking usually forms from the preexisting network of through–splat microcracks, seen in Fig. 2 a).

3.4. Characteristics of black fracture

Fig. 4 b) shows black fracture in a specimen subjected to 300 cycles of TCF. The fracture has occurred mainly in the TGO/TC interface, except at bulky oxide clusters which are usually cut through, giving TGO/TGO fracture. In some cases, the fracture has occurred in the BC/TGO interface, revealing the metallic BC. The TCF also gives fractured TGO, as can be seen in Fig. 5. For specimens subjected to 300 cycles of BRT the fracture has occurred entirely in the TGO/TC interface; the thin even TGO layer is left completely intact. Fig. 4 a) shows black fracture in a specimen subjected to 1150 cycles of BRT; compared to BRT 300 cycles, a shift in fracture mechanism can be seen as BRT 1150 cycles, in addition to TGO/TC fracture, gives large areas of BC/TGO fracture. Compared to TCF 300 cycles, the amount of BC/TGO fracture is somewhat larger in the case of BRT 1150 cycles. However, the TGO in BRT 1150 cycles still consists of predominantly Al_2O_3 and cut-through oxide clusters are uncommon.

4. Discussion

Areas of white fracture consist mainly of interlamellar fracture for all heat treatments and heat treatment times, shown in Fig. 2 a). The occasional translamellar fracture that can be found in white parts of the fracture surface is often associated with discontinuities in the microstructure, such as unmelted or partially melted particles, peaks in the BC/TC interface, etc. This, together with the low increase in adhesion for isothermally oxidized specimens, suggests that the inter-splat sintering is rather modest. The

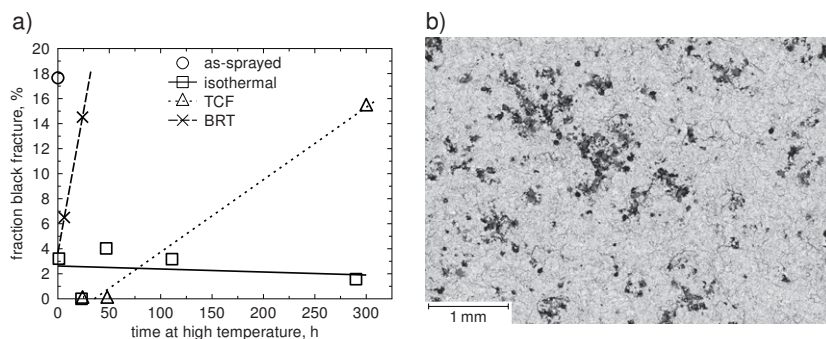


Fig. 3. Fraction of black fracture. a) Fraction black fracture measured by SEM EDS mapping. b) Specimen subjected to TCF 300 cycles, SEM backscatter electron image. Black fracture can be seen as dark areas which are exposed Al_2O_3 .

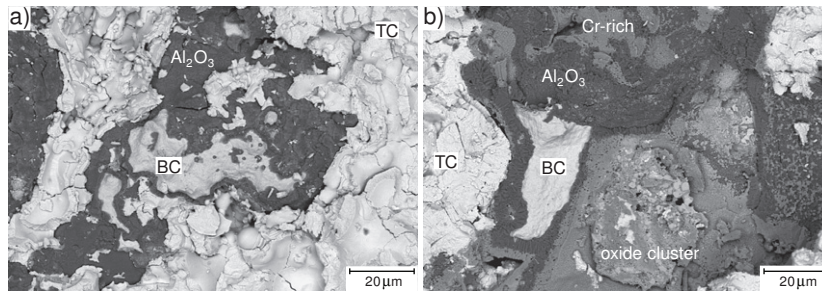


Fig. 4. Characteristics of black fracture, SEM backscatter electron images. a) BRT 1150 cycles. The TGO consists of a thin layer of relatively pure Al_2O_3 , the image shows both TGO/TC and BC/TGO fracture. b) TCF 300 cycles. The image shows TGO/TC and BC/TGO fracture as well as a cut-through oxide cluster. Besides Al_2O_3 and mixed–element oxide clusters, the TGO can be seen to contain colonies of Cr-rich oxides on top of the Al_2O_3 .

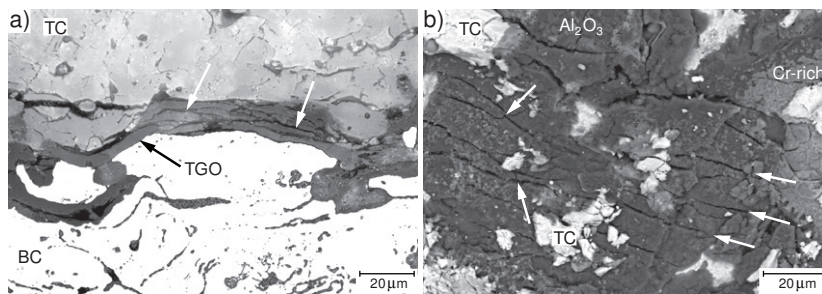


Fig. 5. Damaged interface TGO, marked by arrows, in specimen subjected to 300 cycles of TCF. a) Cross-section, light-optic micrograph. b) Fracture surface after adhesion test, SEM backscatter electron image.

in–splat sintering, however, can be clearly seen on the fracture surfaces as healing of through–splat microcracks.

Specimen subjected to TCF and BRT differ in interface TGO thickness and composition. In the case of BRT, the interface TGO consists of a rather thin and homogeneous layer of Al_2O_3 , whereas the TCF-subjected specimens show a much thicker interface TGO with varying composition: the Al_2O_3 -layer are, at many places, broken by clusters of Cr-rich oxides or mixed–element–oxides, and cut-through oxide clusters can be seen in the black parts of the fracture surface. However, the increase in TGO thickness and the increase in porous oxide clusters alone does not cause a transition from white to black fracture as demonstrated by the isothermal oxidation which gives white fracture for all times. The shift in fracture mechanism between as-sprayed specimens, which gives mixed fracture, and isothermally oxidized specimens, which gives white fracture, is taken as an indication that the development of TGO has some beneficial effects on the adhesion of TBC, [9].

The two cyclic heat treatments give increasing amounts of black fracture with number of cycles. In the case of TCF, the transition from white to mixed fracture is attributed to an increase in interface damage, as can be seen for a cross-section in Fig. 5 a) and on the fracture surface in Fig. 5 b). In the case of BRT, no substantial interface damage can be detected, (in cross-sectioned specimens), even after 1150 cycles; some cracks can be seen in the TC, but this damage does not differ significantly from what can be found in the TCF-subjected specimens. BRT or BRT-like heat treatment typically gives fracture in the TC rather than in the BC/TC interface, [10], so the lack of interface damage is expected. The areas that consist of black fracture is mainly TGO/TC fracture for both BRT and TCF, (in the case of TCF some TGO/TGO

fracture occurs at oxide clusters). However, some BC/TGO fracture can also be seen; such areas are visible in Fig. 4, where they can be seen as brighter areas in the dark Al₂O₃ layer. For BRT a shift in fracture mechanism can be seen as BRT 300 cycles gives TGO/TC fracture only while BRT 1150 cycles gives some BC/TGO fracture.

5. Conclusions

Adhesion tests have been conducted on TBC coated specimens subjected to isothermal heat treatment, thermal cycling fatigue and burner rig test. Isothermally oxidized specimens give fracture in the TC whereas cyclic heat treatment gives increasing amount of BC/TC interface fracture with increasing number of cycles. For TCF a shift from white to mixed fracture occurs somewhere between 48 and 300 cycles. For BRT, a shift from TGO/TC fracture to TGO/TC + BC/TGO fracture occurs with increasing number of cycles.

Acknowledgements

This research has been funded by the Swedish Energy Agency, Siemens Industrial Turbomachinery AB, Volvo Aero Corporation, and the Royal Institute of Technology through the Swedish research program TURBO POWER, the support of which is gratefully acknowledged. The authors would also like to accentuate the contribution of Professor Sören Sjöström who participates in the ongoing TBC research at Linköpings universitet.

References

- [1] P. Bengtsson. *Microstructural, residual stress and thermal shock studies of plasma sprayed ZrO₂-based thermal barrier coatings*. Ph.D. thesis: Linköpings universitet; 1997.
- [2] H. Brodin. *Failure of thermal barrier coatings under thermal and mechanical fatigue loading: Microstructural observations and modelling aspects*. Ph.D. thesis: Linköpings universitet; 2004.
- [3] W. Chen, X. Wu, B. Marple, R. Lima, P. Patnaik. Pre-oxidation and tgo growth behaviour of an air-plasma-sprayed thermal barrier coating. *Surf. Coat. Technol.* 2008;**202**:3787–3796.
- [4] M. Hadad, G. Margot, P. Démarécaux, D. Chicot, J. Lesage, L. Rohr, et al. Adhesion tests of thermal spray coatings: correlation of bond strength and interfacial toughness. *Surf. Eng.* 2007;**23**:279–283.
- [5] P. F. Zhao, C. A. Sun, X. Y. Zhu, F. L. Shang, C. J. Li. Fracture toughness measurements of plasma-sprayed thermal barrier coatings using a modified four-point bending method. *Surf. Coat. Technol.* 2010;**204**:4066–4074.
- [6] M. Gell, E. Jordan, K. Vaidyanathan, K. McCarron, B. Barber, Y.-H. Sohn, et al. Bond strength, bond stress and spallation mechanisms of thermal barrier coatings. *Surf. Coat. Technol.* 1999;**120-121**:53–60.
- [7] R. Vaßen, F. Cernushi, G. Rizzi, A. Scrivani, N. Markocsan, L. Östergren, et al. Recent activities in the field of thermal barrier coatings including burner rig testing in the european union. *Adv. Eng. Mater.* 2008;**10**:907–921.
- [8] ASTM. *Standard C633: Standard Test Method for Adhesion or Cohesion Strength of Thermal Spray Coatings*. ASTM International; 2008.
- [9] N. Markocsan, P. Nylén, J. Wigren, X.-H. Li, A. Tricoire. Effect of thermal aging on microstructure and functional properties of zirconia-base thermal barrier coatings. *J. Therm. Spray Technol.* 2009;**18(2)**:201–208.
- [10] O. Trunova, T. Beck, R. Herzog, R. W. Steinbrech, L. Singheiser. Damage mechanisms and lifetime behavior of plasma sprayed thermal barrier coating systems for gas turbines – part I: Experiments. *Surf. Coat. Technol.* 2008;**202**:5027–5032.